

Peristaltic Transport with Convective Conditions of Heat and Mass Transfer

F. M. Abbasi^{1†}, T. Hayat^{2,3} and A. Alsaedi³

¹Department of Mathematics, COMSATS Institute of Information Technology, Islamabad 44000, Pakistan

²Department of Mathematics, Quaid-I-Azam University 45320, Islamabad 44000, Pakistan

³Nonlinear Analysis and Applied Mathematics (NAAM) Research Group, Faculty of Science, King Abdulaziz University, Jeddah 21589, Saudi Arabia

†Corresponding Author Email: abbasisarkar@gmail.com

(Received January 25, 2014; accepted September 1, 2015)

ABSTRACT

The objective of present communication is to discuss the effect of mass convective condition on the peristaltic transport of viscous fluid in an asymmetric channel. Analysis has been carried out in the presence of Soret and Dufour effects. Comparative study of temperature and concentration fields in the presence and absence of convective conditions through heat and mass transfer is carefully examined. Numerical values of heat and mass transfer rates are computed and analyzed.

Keywords: Convective mass condition; Soret and dufour effects; Comparative analysis.

NOMENCLATURE

$d_1 + d_2$	width of the channel	c	speed of the peristaltic wave
\bar{H}_1	upper wall	\bar{H}_2	lower wall
a_1	amplitude of the wave at d_1	b_1	amplitude of the wave at d_2
λ	wavelength of the peristaltic waves	α	phase difference of the waves
\bar{U}	\bar{X} -component of the velocity	\bar{V}	\bar{Y} -component of the velocity
\bar{t}	time	Subscripts	derivative w.r.t the mentioned component
ρ	density of the fluid	\bar{P}	dimensional pressure
ν	kinematic viscosity	C_p	specific heat and constant pressure
\bar{T}	dimensional temperature	K	thermal conductivity
Φ	dimensional heat generation/absorption	D	mass diffusivity
K_T	thermal diffusion ratio	T_m	mean fluid temperature
C_s	concentration susceptibility	C	dimensional concentration
Lower case letters with overbar ($\bar{u}, \bar{v}, \bar{p}$ etc)	quantities in the moving frame of reference (\bar{x}, \bar{y})	Lower case letters without overbar (u, v, p etc)	dimensionless quantities in the moving frame of reference (x, y)
δ	Wave number	$h_{1,2}$	dimensionless peristaltic walls
d	channel width ratio	a	amplitude ratio for upper wall
b	amplitude ratio for lower wall	Re	reynolds number
θ	dimensionless temperature	$T_{0,1}$	temperature at upper and lower walls respectively
$C_{0,1}$	concentration at upper and lower walls	ϕ	dimensionless concentration

	respectively		
β	dimensionless heat generation/absorption parameter	Br	Brinkman number
Pr	Prandtl number	E	Eckert number
D_f	Dufour number	Sc	Schmidth number
Sr	Soret number	ψ	stream function
Q	dimensional flow rate in the fixed frame	q	dimensional flow rate in the moving frame
η	dimensionless flow rate in the fixed frame	F	dimensionless flow rate in the moving frame
\bar{Q}	time averaged mean flow rate	$L_{1,2}$	wall heat transfer coefficients for upper and lower walls respectively
$k_{m1,2}$	wall mass transfer coefficients for upper and lower walls respectively	$Bt_{1,2}$	heat transfer Biot numbers for the upper and lower walls respectively
$ML_{1,2}$	mass transfer Biot numbers for the upper and lower walls respectively		

1. INTRODUCTION

There is growing interest of the recent investigators in the interaction of heat transfer with peristaltic motion. Such interest in fact stems because of relevance of such topic in physiology and industry. In particular the peristalsis through heat transfer is important in hemodialysis and oxygenation, cancer tumor treatment, tissue engineering, nuclear reactors, power generators and biomedical engineering. The simultaneous effects of heat and mass transfer are further important because oxygen and nutrients diffuse out of the blood vessels to the neighboring tissues. Although information on peristalsis with heat/mass transfer is quite sizeable but some recent contributions in this direction may be seen through the studies Mekheimer *et al.* (2008, 2010), Nadeem *et al.* (2009), Hayat *et al.* (2011, 2014, 2014a), Abbasi *et al.* 2014a, 2015b, Tripathi (2012) and Ali *et al.* (2010). In these preceding studies, the heat/mass transfer effects are not analyzed through convective wall conditions. Very few attempts have been recently made for the peristaltic flows with convective heat transfer conditions. The relevant works in this direction are by Abbasi *et al.* (2014b, 2015b, 2015c).

The main interest here is to examine the peristaltic flow in an asymmetric channel with convective mass condition. Problem formulation is made in presence of Soret and Dufour effects. Long wavelength and low Reynolds number assumptions are employed. Attention is focused to the exact solutions of temperature and concentration fields in presence/absence of convective heat and mass transfer conditions. This paper is organized as follows. Section two consists of flow equations and boundary conditions. The solution expressions are presented in section three. Section four analyzes the impact of pertinent parameters. Main observations are included in section five.

2. MATHEMATICAL ANALYSIS

Consider the peristaltic waves traveling along the walls of an asymmetric channel of width $d_1 + d_2$. An incompressible viscous fluid fills the space inside the channel. We select coordinate system in such a manner that \bar{X} -axis lies along the length of the channel and the \bar{Y} -axis is taken normal to \bar{X} -axis. The peristaltic waves travel on the channel walls in the \bar{X} direction with speed c . The wall shapes are given as follows:

$$\bar{H}_1(\bar{X}, \bar{t}) = d_1 + a_1 \cos\left(\frac{2\pi}{\lambda}(\bar{X} - c\bar{t})\right),$$

upper wall,

$$\bar{H}_2(\bar{X}, \bar{t}) = -d_2 - b_1 \cos\left(\frac{2\pi}{\lambda}(\bar{X} - c\bar{t}) + \alpha\right),$$

lower wall.

In above relations a_1 and b_1 are the amplitudes of the waves for upper and lower walls respectively, λ is the wavelength and α is the phase difference of the waves. These waves are responsible for the disturbance in the channel. The equation of conservation of mass for two-dimensional incompressible flow is

$$\bar{U}_{\bar{X}} + \bar{V}_{\bar{Y}} = 0. \tag{2}$$

Here \bar{U} and \bar{V} are the longitudinal and transverse components of velocity. The scalar equations through momentum equation are

$$\bar{U}_t + \bar{U}\bar{U}_{\bar{X}} + \bar{V}\bar{U}_{\bar{Y}} = -\frac{1}{\rho}\bar{P}_{\bar{X}} + \nu[\bar{U}_{\bar{X}\bar{X}} + \bar{U}_{\bar{Y}\bar{Y}}] \tag{3}$$

$$\bar{V}_t + \bar{U}\bar{V}_{\bar{X}} + \bar{V}\bar{V}_{\bar{Y}} = -\frac{1}{\rho}\bar{P}_{\bar{Y}} + \nu[\bar{V}_{\bar{X}\bar{X}} + \bar{V}_{\bar{Y}\bar{Y}}] \tag{4}$$

where ρ , \bar{P} , \mathbf{v} and \bar{t} indicate the density, pressure, kinematic viscosity and time respectively. Subscripts denote the partial derivatives. Laws of energy and concentration yield

$$C_p(\bar{T}_t + \bar{U}\bar{T}_X + \bar{V}\bar{T}_Y) = \frac{K}{\rho}[T_{XX} + T_{YY}] + \frac{\Phi}{\rho} + \mathbf{v} \left[2\left(\bar{U}^2 + \bar{V}^2\right) + (\bar{U}\bar{V} + \bar{V}\bar{X})^2 \right] + \frac{DK_T}{\rho C_s} [C_{XX} + C_{YY}] \quad (5)$$

$$C_t + \bar{U}C_X + \bar{V}C_Y = D[C_{XX} + C_{YY}] + \frac{DK_T}{T_m} [T_{XX} + T_{YY}] \quad (6)$$

Here the second term on right side of Eq. (5) is the heat generation/absorption term, third term is due to consideration of viscous dissipation and the last term is due to Dufour effect. Further C_p is the specific heat at constant pressure, T the temperature, K the thermal conductivity of the fluid, D the mass diffusivity, K_T the thermal diffusion ratio, C_s the concentration susceptibility, C the concentration and T_m the fluid mean temperature. In order to transform our problem from the fixed frame (laboratory frame) to a frame of reference moving with the wave with speed C (wave frame) we use the following transformations:

$$\bar{x} = \bar{X} - ct, \quad \bar{y} = \bar{Y}, \quad \bar{u} = \bar{U} - c, \quad \bar{v} = \bar{V}, \quad \bar{p}(\bar{x}, \bar{y}) = \bar{P}(\bar{X}, \bar{Y}, t), \quad (7)$$

in which \bar{u} , \bar{v} and \bar{p} are the velocity components and pressure in wave frame (\bar{x}, \bar{y}) . Considering the dimensionless quantities

$$\begin{aligned} x &= \frac{\bar{x}}{\lambda}, \quad y = \frac{\bar{y}}{d_1}, \quad u = \frac{\bar{u}}{c}, \quad v = \frac{\bar{v}}{c\delta}, \quad \delta = \frac{d_1}{\lambda}, \quad H_1 = \frac{\bar{H}_1}{d_1}, \\ H_2 &= \frac{\bar{H}_2}{d_1}, \quad d = \frac{d_2}{d_1}, \quad a = \frac{a_1}{d_1}, \quad b = \frac{b_1}{d_1}, \quad p = \frac{d_1^2 \bar{p}}{c\lambda\mu}, \quad \mathbf{v} = \frac{\mu}{\rho}, \\ \text{Re} &= \frac{\rho c d_1}{\mu}, \quad t = \frac{ct}{\lambda}, \quad \theta = \frac{T - T_0}{T_1 - T_0}, \quad \phi = \frac{C - C_0}{C_1 - C_0}, \\ \beta &= \frac{\Phi}{KT_0}, \quad Br = \text{Pr} E, \quad E = \frac{c^2}{C_p(T_1 - T_0)}, \quad \text{Pr} = \frac{\mu C_p}{K}, \\ Sr &= \frac{\rho DK_T(T_1 - T_0)}{\mu T_m(C_1 - C_0)}, \quad Sc = \frac{\mu}{\rho D}, \quad D_f = \frac{D(C_1 - C_0)K_T}{C_s C_p \mu(T_1 - T_0)}, \\ u &= \psi_y, \quad v = -\psi_x. \end{aligned} \quad (8)$$

and applying the long wavelength and low Reynolds number approximations we have

$$p_x = \psi_{yyy}, \quad (9)$$

$$p_y = 0, \quad (10)$$

$$\theta_{yy} + Br(\psi_{yy})^2 + \text{Pr} D_f(\phi_{yy}) + \beta = 0, \quad (11)$$

$$\frac{1}{Sc}\phi_{yy} + Sr\theta_{yy} = 0, \quad (12)$$

where continuity equation is identically satisfied, μ denotes the dynamic viscosity, ψ the stream function, Re the Reynolds number, Br the Brinkman number, E the Eckret number, Pr the Prandtl number, δ the wave number, ϕ dimensionless concentration, θ the dimensionless temperature, T_0 , C_0 the temperature and concentration of the upper wall and T_1 , C_1 the temperature and concentration of the lower wall respectively. Equation (10) also indicates that $p \neq p(y)$.

Taking \bar{H}_i ($i=1,2$) as functions of \bar{X} and \bar{t} , the dimensionless volume flow rate in laboratory frame is

$$Q = \int_{H_2}^{\bar{H}_1} \bar{U}(\bar{X}, \bar{Y}, t) dY \quad (13)$$

and in wave frame we have

$$q = \int_{h_2}^{h_1} u(x, y) dy, \quad (14)$$

in which h_i ($i=1,2$) are functions of X alone. From Eqs. (8) (13) and (14) we can write

$$Q = q + ch_1(x) - ch_2(x). \quad (15)$$

The time averaged flow over a period T_f is given by

$$\bar{Q} = \frac{1}{T_f} \int_0^{T_f} Q dt, \quad (16)$$

which implies that

$$\bar{Q} = q + cd_1 - cd_2. \quad (17)$$

Defining η and F as the dimensionless mean flows in laboratory and wave frames by

$$\eta = \frac{\bar{Q}}{cd_1}, \quad F = \frac{q}{cd_1}, \quad (18)$$

and using Eqs. (16) and (18) one has

$$\eta = F + 1 + d, \quad (19)$$

where

$$F = \int_{h_2}^{h_1} \frac{\partial \psi}{\partial y} dy. \quad (20)$$

The convective boundary condition for the temperature is defined as follows:

$$-K \frac{\partial T}{\partial Y} = l(T - T_w),$$

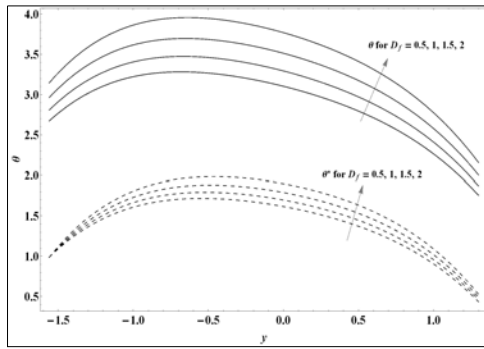


Fig. 1 (a)

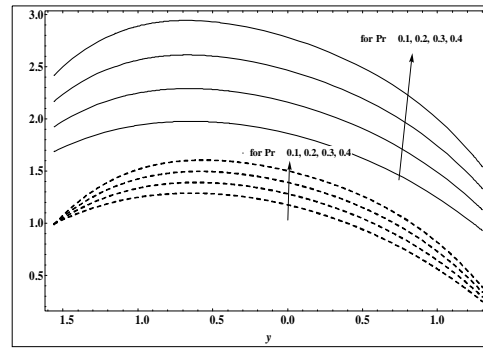


Fig. 1 (b)

Fig. 1. Effects of D_f and Pr on the temperature profile θ and θ^* when $\eta = 1.6$, $a = 0.5$, $b = 0.4$, $\beta = 0.5$, $d = 1.2$, $Sc = 0.5$, $Sr = 0.5$, $Bi_1 = 2$ and $Bi_2 = 1$.

in which K is the thermal conductivity, l is the wall heat transfer coefficient and T_w is the temperature of the wall. This condition includes in form of heat transfer coefficient l the material properties of the wall into the problem of heat transfer. The asymmetry of channel demands to choose different heat transfer coefficients for the upper and lower walls, i.e. l_1 for the upper and l_2 for the lower wall. We can also check the behavior of temperature when $l_1 = l_2$. Analogues to the heat transfer at the boundary we use the condition for the mass transfer

$$-D \frac{\partial C}{\partial Y} = k_m (C - C_w).$$

Here k_m is the mass transfer coefficient. Such coefficient is used to describe the ratio between actual mass flux of a species into or out of the flowing fluid and the driving force that causes such flux and C_w the concentration at the wall.

The dimensionless boundary conditions can be expressed as follows:

$$\begin{aligned} \psi &= \frac{F}{2}, \quad \psi_y = -1, \quad \theta_y + Bi_1 \theta = 0, \quad \phi_y + Mi_1 \phi = 0, \quad \text{at } y = h_1, \\ \psi &= -\frac{F}{2}, \quad \psi_y = -1, \quad \theta_y - Bi_2 (\theta - 1) = 0, \quad \phi_y - Mi_2 (\phi - 1) = 0, \\ &\text{at } y = h_2, \end{aligned} \tag{21}$$

where

$$\begin{aligned} h_1(x) &= 1 + a \cos(2\pi x), \quad h_2(x) = -d - b \cos(2\pi x + \alpha), \\ Bi_1 &= \frac{l_1 d_1}{K}, \quad Bi_2 = \frac{l_2 d_1}{K}, \quad Mi_1 = \frac{k_{m1} d_1}{D} \quad \text{and} \quad Mi_2 = \frac{k_{m2} d_1}{D}. \end{aligned} \tag{22}$$

In above equations l_1 , l_2 , k_{m1} , and k_{m2} are the dimensionless transfer coefficients, $Bi_{1,2}$ are heat transfer Biot-numbers and $Mi_{1,2}$ are the mass transfer Biot-numbers.

3. SOLUTION EXPRESSIONS

Now we consider the following two cases.

Case I: With convective condition at the boundary

The obtained closed form solutions for the temperature and concentration are given by

$$\theta = \frac{1}{(2(-1+A)(h_1-h_2)^6 (Bi_1 + Bi_2 + Bi_1 Bi_2 h_1 - Bi_1 Bi_2 h_2)) \times (12Br(F+h_1-h_2)^2 (A_1 + A_2 - A_3 y + A_4 y^2 - A_5 y^3 + A_5 y^4) + A_6)}$$

$$\phi = \frac{1}{2(-1+A)(h_1-h_2)^6 (Mi_1 + Mi_2 + (h_1-h_2)Mi_1 Mi_2) (-A_{10} - A_{12} + A_{13} + A_{15} \beta + A_{16} + h_1^7 A_{18})}$$

Case II: Without convective condition at the boundary

In this case the physical quantities are denoted by asterisk. The resulting problems here are

$$\psi_{yyyy}^* = 0, \tag{23}$$

$$\theta_{yy}^* + Br(\psi_{yy}^*)^2 + Pr D_f (\phi_{yy}^*) + \beta = 0, \tag{24}$$

$$\frac{1}{Sc} \phi_{yy}^* + Sr \theta_{yy}^* = 0, \tag{25}$$

$$\psi^* = \frac{F}{2}, \quad \psi_y^* = -1, \quad \theta^* = 0, \quad \phi^* = 0, \quad \text{at } y = h_1, \tag{26}$$

$$\psi^* = -\frac{F}{2}, \quad \psi_y^* = -1, \quad \theta^* = 1, \quad \phi^* = 1, \quad \text{at } y = h_2.$$

The solutions can be presented into the following forms:

$$\theta^* = \frac{h_1 - y}{2(h_1 - h_2)^6 (-1 + A) (B_1 - y B_2 + y^2 B_3 - y^3 B_4 + (h_1 - h_2)^6 (h_2 - y) \beta)}$$

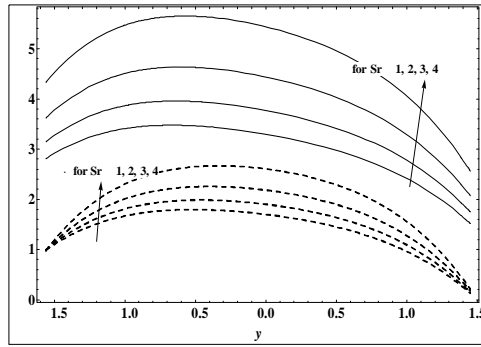


Fig. 2 (a)

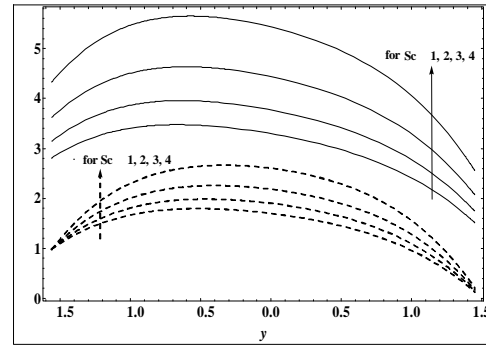


Fig. 2 (b)

Fig. 2. Effects of Sc and Sr on the temperature profile θ and θ^* when $\eta=1.6$, $a=0.5$, $b=0.4$, $\beta=0.5$, $d=1.2$, $Pr=0.5$, $D_f=0.5$, $Bi_1=2$ and $Bi_2=1$.

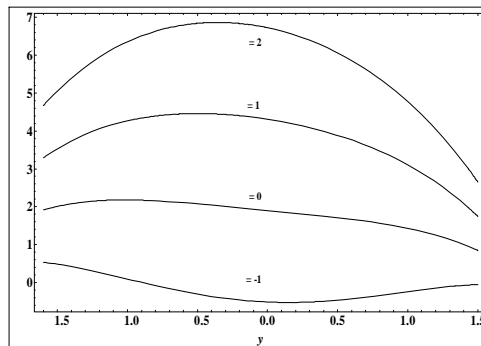


Fig. 3 (a)

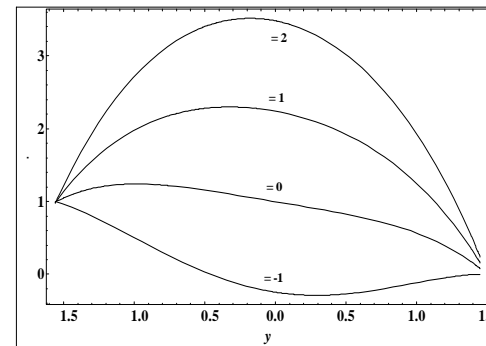


Fig. 3 (b)

Fig. 3. Effect of β on the temperature profile θ and θ^* when $\eta=1.6$, $a=0.5$, $b=0.4$, $Sc=0.5$, $d=1.2$, $Pr=0.5$, $D_f=0.5$, $Bi_1=2$ and $Bi_2=1$.

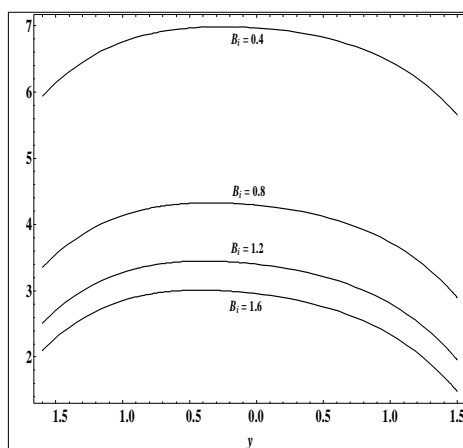


Fig. 4. Effect of Bi on the temperature profile θ when $\eta=1.6$, $a=0.5$, $b=0.4$, $Sc=0.5$, $d=1.2$, $Pr=0.5$, $Sr=0.5$, $\beta=0.5$, and $D_f=0.5$.

$$\phi^* = \frac{h_1 - y}{2(h_1 - h_2)^6(-1 + A)} (B_5 + yB_6 + y^2B_7 + B_8y^3 - (h_1 - h_2)^6 ScSr(h_2 - y)\beta)$$

The values of A_i s and B_i s appearing in the solution expressions can be obtained by the usual computations.

4. RESULTS AND DISCUSSION

Our interest in this section is to analyze the behavior of influential parameters. Plots are presented and analyzed for θ , θ^* , ϕ and ϕ^* . A comparative study in presence and absence of convective condition is made. Also the impact of Biot-numbers is examined. Two tables are given for the numerical values of transfer rates at the upper wall.

Fig. 1 (a & b) are plotted for the variations of D_f and Pr on θ . It is found that temperature is large when compared to θ^* . Consideration of convective boundary condition (for fixed values of

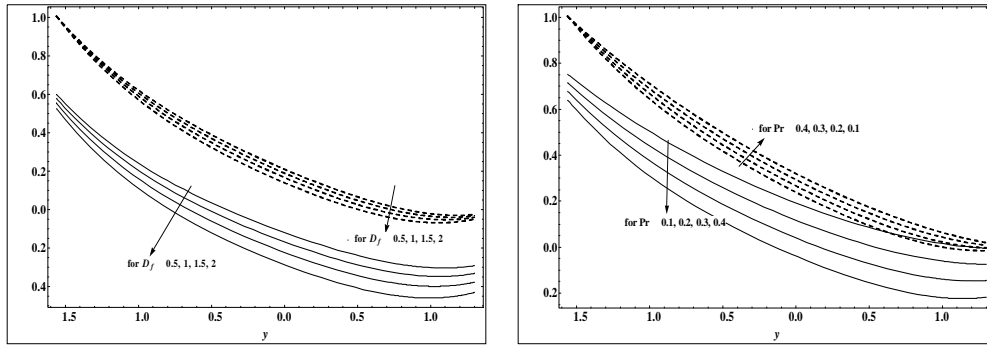


Fig. 5. Effect of D_f and Pr on the concentration profile ϕ and ϕ^* when $\eta = 1.6$, $a = 0.5$, $b = 0.4$, $\beta = 0.5$, $d = 1.2$, $Sc = 0.5$, $Sr = 0.5$, $Mi_1 = 1$ and $Mi_2 = 2$.

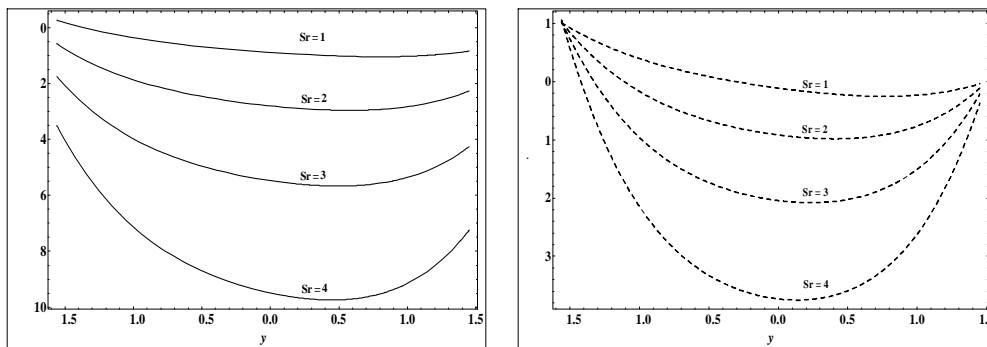


Fig. 6. Effect of Sr on the concentration profile ϕ and ϕ^* when $\eta = 1.6$, $a = 0.5$, $b = 0.4$, $\beta = 0.5$, $d = 1.2$, $Sc = 0.5$, $Pr = 0.5$, $Mi_1 = 1$ and $Mi_2 = 2$.

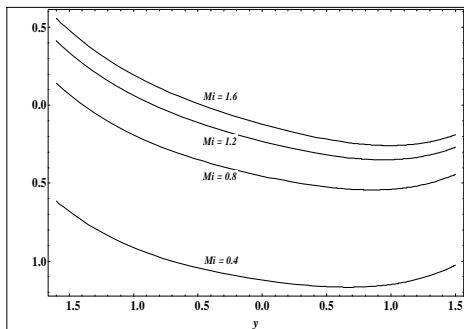


Fig. 7. Effect of Mi on the concentration profile ϕ when $\eta = 1.6$, $a = 0.5$, $b = 0.4$, $\beta = 0.5$, $d = 1.2$, $Sc = 0.5$ and $Sr = 0.5$.

Bi_1 and Bi_2) does not affect the behavior of any parameter on the temperature. However the temperature increases in the Figs. 1-3. It is found that the temperature increases by increasing D_f , Pr, Sr, Sc and β . Fig. 4 showed that the temperature profile is decreasing function of heat transfer Biot number.

Figs. 5-7 are plotted to analyze the behavior of concentration profile for different parameters. The

dimensionless concentration profile is found to decrease with an increase in D_f , Pr and Sr. Such decrease is large for the case of Sr when compared with D_f and Pr. The concentration field in presence of convective mass condition has been noted less than in its absence.

Numerical values for the heat transfer rate at the upper wall are given in Table 1. It is found that heat transfer rate at the upper wall is increased with an increase in Dufour, Prandtl and Soret numbers. Values of θ' are relatively higher than the values of $(\theta^*)'$ at the boundary. It means that the transfer rate is higher when one takes into account the convective heat transfer at the boundary. Further, the heat transfer rate is an increasing function of heat transfer Biot number.

Table 2 has been prepared for the concentration transfer rate at the upper wall. Such rate increases through an increase in D_f , Pr and Sr. For Dufour number the value of ϕ' is greater than that of $(\phi^*)'$, but when Pr and Sr are increased the value of ϕ' decreases by a small amount. It is also noticed that increasing the value of mass transfer

Biot-number decreases the transfer rate at the boundary.

Table 1 Effects of various parameters on heat transfer rate at the upper wall

D_f	Pr	Sr	Bi_1	Bi_2	$-\theta'(h_1)$	$-(\theta^*)'(h_1)$
0.5	0.5	0.5	2.0	1.0	2.74048	2.60257
1.0					2.91983	2.76344
1.5					3.12676	2.94905
2.0					3.36818	3.16561
0.5	0.5				2.74048	2.60257
	1.0				4.70102	4.36114
	1.5				6.96317	6.39025
	2.0				9.60235	8.75755
	0.5	0.5			2.74048	2.60257
		1.0			2.91983	2.76344
		1.5			3.12676	2.94905
		2.0			3.36818	3.16561
		0.5	1	1	2.45817	–
			2	2	2.51163	–
			3	3	2.53621	–
			4	4	2.55032	–

Table 2 Effects of various parameters on mass transfer rate at the upper wall

D_f	Pr	Sr	Mi_1	Mi_2	$\phi'(h_1)$	$(\phi^*)'(h_1)$
0.5	0.5	0.5	1	3	0.2345420	0.212593
1.0					0.2683550	0.252809
1.5					0.30737	0.299213
2.0					0.3528880	0.353351
0.5	0.5				0.2345420	0.212593
	1.0				0.60418	0.652234
	1.5				1.03069	1.15951
	2.0				1.52828	1.75134
	0.5	0.5			0.2345420	0.212593
		1.0			0.7755510	0.856059
		1.5			1.39979	1.59852
		2.0			2.12807	2.46472
		0.5	1	1	0.356998	–
			2	2	0.303532	–
			3	3	0.27896	–
			4	4	0.264842	–

5. CONCLUSIONS

The peristaltic flow with convective conditions of heat and mass transfer is addressed. The main results can be summarized as follows:

- There is enhancement of temperature in presence of convective heat transfer condition.
- Effect of convective mass condition is to decrease a concentration field.
- Heat transfer rate at the boundary is higher in presence of convective condition.
- Heat transfer rate at the boundary increases with an increase in the heat transfer Biot number Bi .
- The mass transfer rate at the boundary decreases by increasing Mi .

REFERENCES

Abbasi, F. M., T. Hayat and B. Ahmad (2014). Peristaltic flow in an asymmetric channel with convective boundary conditions and Joule heating. *Journal of Central South University* 21, 1411-1416.

Abbasi, F. M., T. Hayat and B. Ahmad (2015). Peristaltic flow with convective mass condition and thermal radiation. *Journal of Central South University* 22, 2369-2375.

Abbasi, F. M., T. Hayat and A. Alsaedi (2015). Numerical analysis for peristaltic motion of MHD Eyring-Prandtl fluid in an inclined asymmetric channel with inclined magnetic field. *Journal of Applied Fluid Mechanics, in press*.

Abbasi, F. M., T. Hayat, A. Alsaedi and B. Ahmed (2014). Soret and Dufour effects on peristaltic transport of MHD fluid with variable viscosity. *Applied Mathematics and Information Sciences*. 8, 211-219.

Abbasi, F. M., T. Hayat and B. Ahmad (2015). Peristaltic transport of an aqueous solution of silver nanoparticles with convective heat transfer at the boundaries. *Canadian Journal of Physics* 93, 1-9.

Ali, N., M. Sajid, T. Javed and Z. Abbas (2010). Heat transfer analysis of peristaltic flow in a curved channel. *International Journal of Heat and Mass Transfer* 53, 3319-3325.

Hayat, T., F. M. Abbasi and A. A. Hendi (2011). Heat transfer analysis for peristaltic mechanism in variable viscosity fluid. *Chinese Physics Letters*. 28, 044701.

Hayat, T., F. M. Abbasi, M. S. Alhuthali, B. Ahmad and G. Q. Chen (2014). Soret and Dufour effects on the peristaltic transport of a third order fluid. *Heat Transfer Research* 45, 589-602.

Hayat, T., F. M. Abbasi and A. Alsaedi (2014). Soret and Dufour effects on peristaltic flow in an asymmetric channel. *Arabian Journal of Science and Engineering* 39, 4341-4349.

Mekheimer, Kh. s., S. Z. A. Husseny and Y. Abd Elmaboud (2010). Effects of heat transfer and

- space porosity on peristaltic flow in a vertical asymmetric channel. *Numerical Methods for Partial Differential Equations* 26, 747-770.
- Mekheimer, S. Kh. and Y. Abd elmaboud (2008). The influence of heat transfer and magnetic field on peristaltic transport of a Newtonian fluid in a vertical annulus: application of an endoscope. *Physics Letters A* 372, 1657-1665.
- Nadeem, S., T. Hayat, N. S. Akbar and M. Y. Malik (2009). On the influence of heat transfer in peristalsis with variable viscosity. *International Journal of Heat and Mass Transfer* 52, 4722-4730.
- Tripathi, D. (2012). A mathematical model for swallowing of food bolus through the oesophagus under the influence of heat transfer. *International Journal of Thermal Science* 51, 91-101.